

# PNAS

[www.pnas.org](http://www.pnas.org)

Supplementary Information for

A middle Eocene lowland humid subtropical 'Shangri-La' ecosystem in central Tibet

Tao Su, Robert A. Spicer, Fei-Xiang Wu, Alexander Farnsworth, Jian Huang, Cédric Del Rio, Tao Deng, Lin Ding, Wei-Yu-Dong Deng, Yong-Jiang Huang, Alice Hughes, Lin-Bo Jia, Jian-Hua Jin, Shu-Feng Li, Shui-Qing Liang, Jia Liu, Xiao-Yan Liu, Sarah Sherlock, Teresa Spicer, Gaurav Srivastava, He Tang, Paul Valdes, Teng-Xiang Wang, Mike Widdowson, Meng-Xiao Wu, Yao-Wu Xing, Cong-Li Xu, Jian Yang, Cong Zhang, Shi-Tao Zhang, Xin-Wen Zhang, Fan Zhao, Zhe-Kun Zhou

Emails: [sutao@xtbg.org.cn](mailto:sutao@xtbg.org.cn), [zhouzk@xtbg.ac.cn](mailto:zhouzk@xtbg.ac.cn)

**This PDF file includes:**

Figures S1 to S17  
Tables S1 to S4  
SI References



**Fig. S1.** Five collecting locations in the Niubao Formation that yield abundant fossils. Vehicles on the road provide scale. The numbers relate to the fossil horizons indicated by leaf symbols in Fig. 1C.

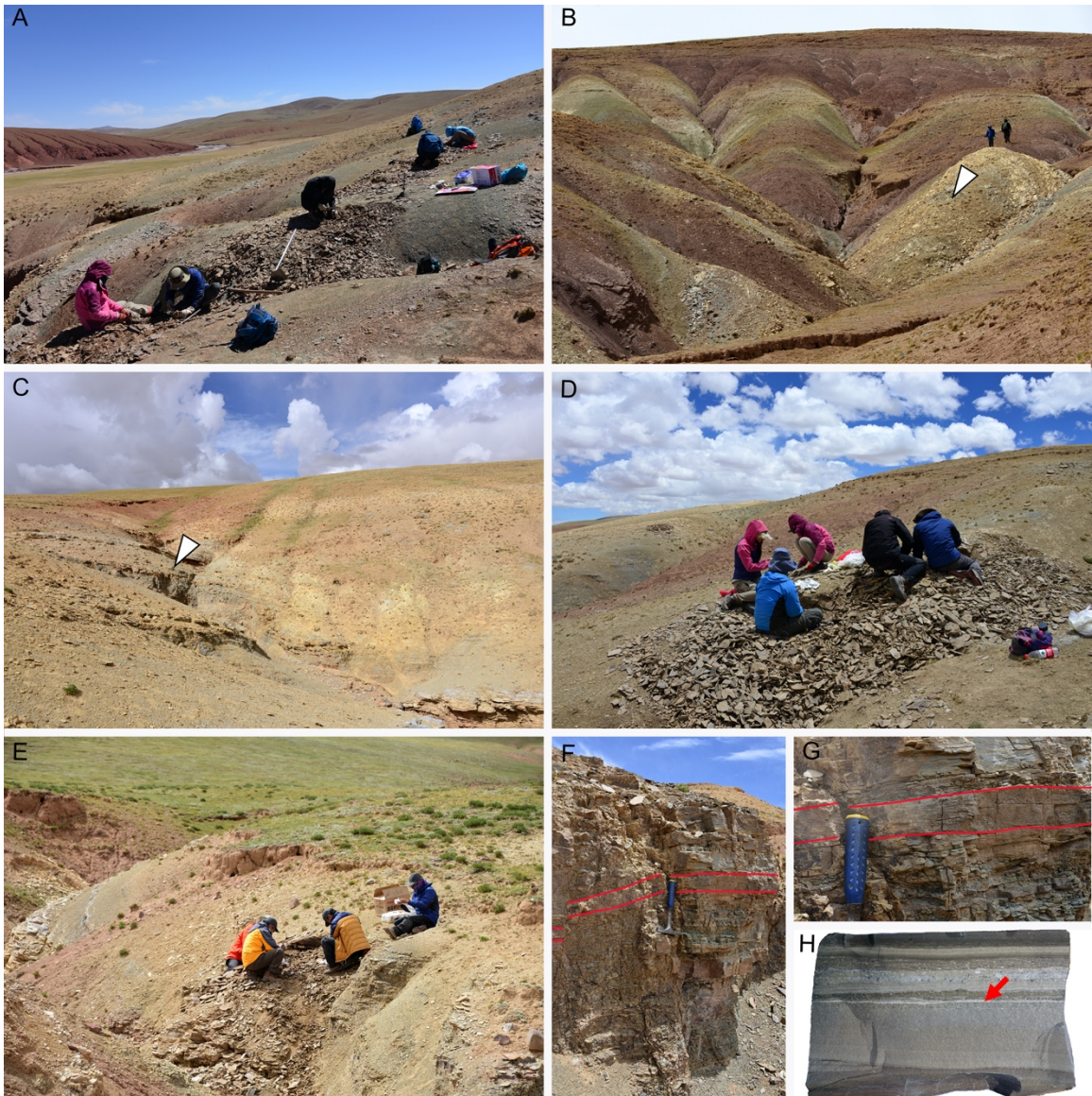


**Fig. S2.** Photos of each fossil-bearing layer in Jianglang village, Bangor Basin, central Tibetan Plateau. (A-E) fossil layers XZBGJL1-5 respectively in this study, the number of each layer corresponds to Fig. 1C and *SI Appendix*, Fig. S1. (F-H) the tephra-rich horizon just below the fossil assemblage XZBGJL5, arrow in red is the layer for radiometric dating.



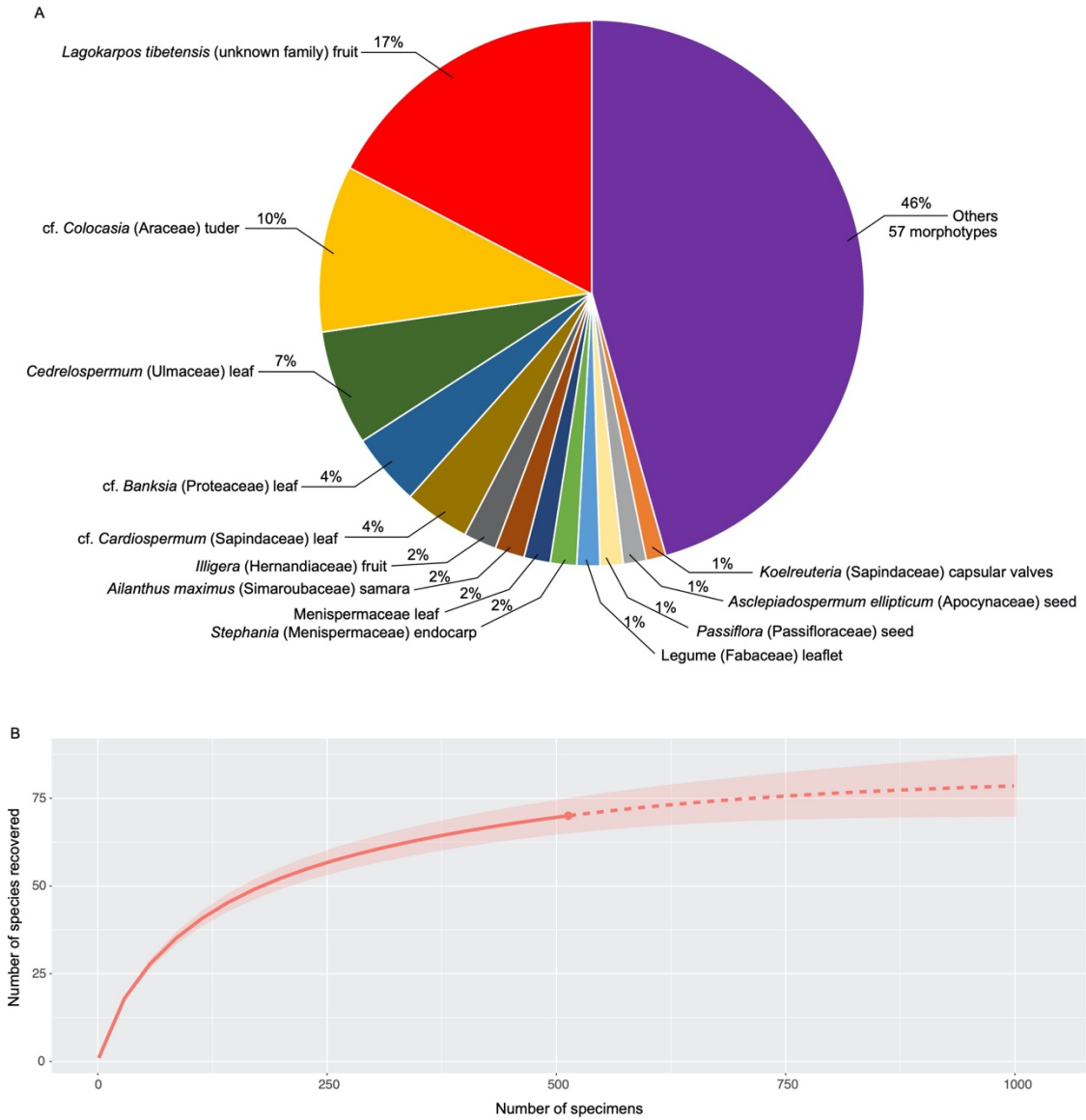


**Fig. S3.** Specimen proportions of plant groups in the Jianglang flora (A), and a rarefaction curve illustrating the rate of increase in species discovery with increasing specimen collection (B). The solid line indicates sampling to date, please note that the number of specimens would increase slightly if more specimens were collected (dash line).



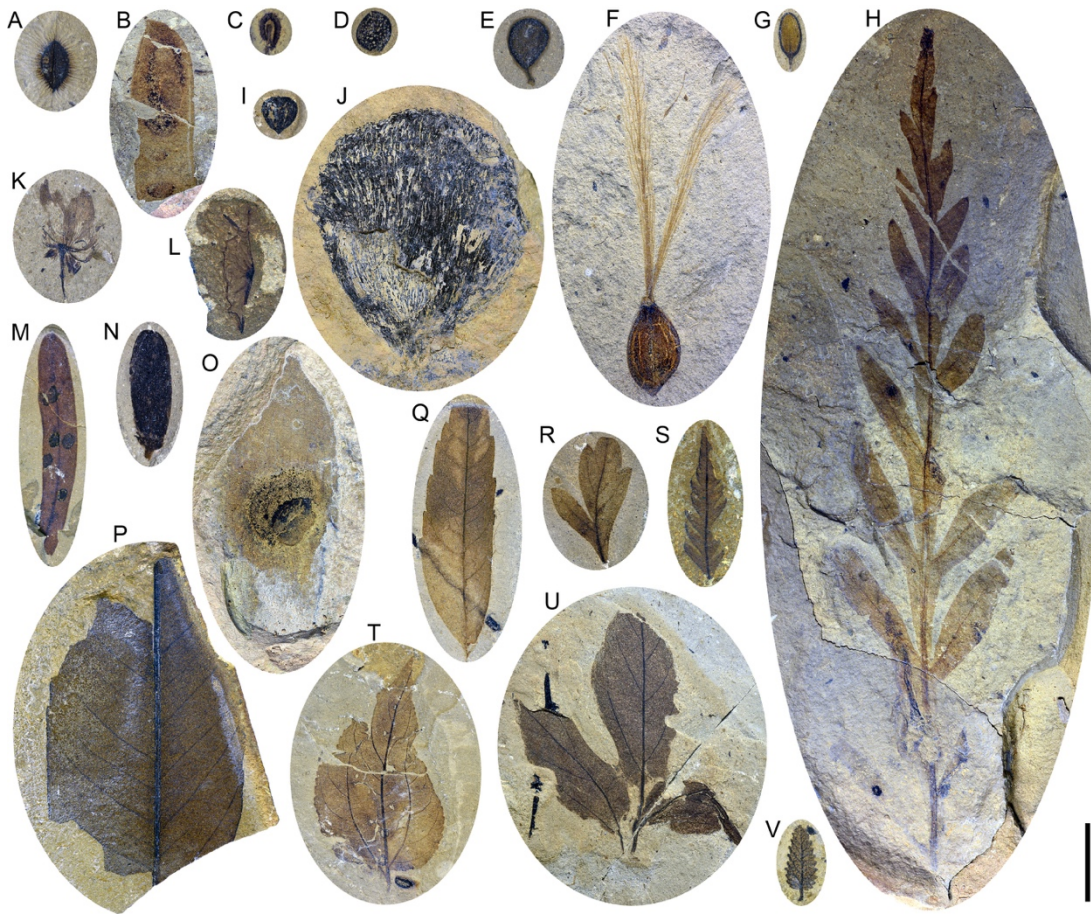


**Fig. S4.** Examples of the diversity of plant taxa from layer No. XZBGJL1 assemblage. (A) *Illigera* (Hernandiaceae) winged fruit, XZBGJL1-0003; (B) Legume (Fabaceae) fruit 1, XZBGJL1-0012; (C) *Stephania* (Menispermaceae) endocarp, XZBGJL1-0021; (D) cf. *Passiflora* (Passifloraceae) seed, XZBGJL1-0007; (E) Unknown obovate fruit, XZBGJL1-0010; (F) *Lagokarpus tibetensis* (unknown familial affinity) winged fruit, XZBGJL1-0383 (1); (G) Unknown long elliptical seed, XZBGJL1-0019; (H) cf. *Lomatia* (Proteaceae) leaf, XZBGJL1-0039; (I) Vitaceae seed, XZBGJL1-0035; (J) cf. *Colocasia* (Araceae) tubers, XZBGJL1-0024; (K) Unknown flower, XZBGJL1-0008; (L) Unknown winged fruit, XZBGJL1-0033; (M) JL1-Leaf-M01, XZBGJL1-0028; (N) Unknown oblong fruit with sepals, XZBGJL1-0022; (O) *Ailanthus maximus* (Simaroubaceae) fruit, XZBGJL1-0009 (2); (P) JL1-Leaf-M02, XZBGJL1-0038; (Q) JL1-Leaf-M03, XZBGJL1-0027; (R) cf. *Cardiospermum* (Sapindaceae) leaf, XZBGJL1-0025; (S) JL5-Leaf-M05, XZBGJL1-0002; (T) *Ziziphus* (Rhamnaceae) leaf, XZBGJL1-0023; (U) JL1-Leaf-M04, XZBGJL1-0013; (V) *Cedrelospermum* (Ulmaceae) leaf, XZBGJL1-0016. Scale bar = 1 cm.



**Fig. S5.** Examples of the diversity of plant taxa from No. XZBGJL2-4 assemblages. (A) *Asclepiadospermum ellipticum* (Apocynaceae) seed, XZBGJL2- 0009 (3). (B) cf. *Colocasia* (Araceae) tubers, XZBGJL2-0001. (C) Sapindaceae leaf, XZBGJL3-0001. (D) cf. *Banksia* (Proteaceae) leaf, XZBGJL3-0002. (E) JL3-Leaf-M01, XZBGJL3-0003. (F) *Cedrelospermum* (Ulmaceae) leaf, XZBGJL3-0004. (G) Unknown fruit with ridges, XZBGJL3-0013. (H) JL3-Leaf-M02, XZBGJL3-0012. (I) JL5-Leaf-M18, XZBGJL3-0006. (J) Unknown small and elongate fruit, XZBGJL3- 0011. (K) Menispermaceae leaf, XZBGJL3-0010. (L) JL3-Leaf-M03, XZBGJL3- 0007. (M) Legume (Fabaceae) fruit 2, XZBGJL3-0009. (N) *Stephania* (Menispermaceae) endocarp, XZBGJL4-0009. (O) cf. *Pachysandra* (Buxaceae) fruit, XZBGJL4-0003. (P) JL4-Leaf-M01, XZBGJL4-0011. Scale bar = 1 cm.





**Fig. S6.** The diversity of plant taxa from No. XZBGJL5 assemblage (for CLAMP analysis). (A) cf. *Banksia* leaf, XTBGJL5-0037. (B) JL5-Leaf-M01, XTBGJL5-0018. (C) cf. *Comptonia* (Myricaceae) leaf, XTBGJL5-0250. (D) cf. *Cardiospermum* leaf (Sapindaceae), XTBGJL5-0348. (E) JL5-Leaf-M02, XTBGJL5-0396. (F) JL5-Leaf-M03, XTBGJL5-0513. (G) *Cedrelospermum* (Ulmaceae) leaf, XTBGJL5-0410. (H) *Macclintockia* (unknown family) leaf, XTBGJL5-0245. (I) JL5-Leaf-M05, XTBGJL5-0532. (J) Fabaceae leaf, XTBGJL5-0123. (K) JL5-Leaf-M06, XTBGJL5-0246. (L) Myrtales leaf, XTBGJL5-0166. (M) JL5-Leaf-M08, XTBGJL5-0266. (N) JL5-Leaf-M09, XTBGJL5-0541. (O) *Syzygioides* (Myrtaceae) leaf, XTBGJL5-0292. (P) JL5-Leaf-M10, XTBGJL5-0049. (Q) JL5-Leaf-M11, XTBGJL5-0244. Scale bar = 1 cm.





**Fig. S7.** The diversity of plant taxa from No. XZBGJL5 assemblage (for CLAMP analysis, continued). (A) JL5-Leaf-M12, XTBGJL5-0235. (B) JL5-Leaf-M13, XTBGJL5-0390. (C) JL5-Leaf-M14, XTBGJL5-0509. (D) JL5-Leaf-M15, XTBGJL5-0542. (E) JL5-Leaf-M16, XTBGJL5-0538. (F) JL5-Leaf-M17, XTBGJL5-0129. (G) JL5-Leaf-M18, XTBGJL5-0279. (H) JL5-Leaf-M19, XTBGJL5-0428. (I) Menispermaceae leaf, XTBGJL5-0195. (J) JL5-Leaf-M20, XTBGJL5-0516. (K) JL5-Leaf-M21, XTBGJL5-0326. (L) JL5-Leaf-M04, XTBGJL5-0055. (M) JL5-Leaf-M07, XTBGJL5-0115. (N) cf. *Ailanthus* (Simaroubaceae) leaf, XTBGJL5-0388. Scale bar = 1 cm.



**Fig. S8.** Examples of plant taxa from No. XZBGJL5 assemblage (non-leaf). (A) *Ailanthus maximus* (Simaroubaceae) fruit, XTBGJL5-0007 (2). (B) *Koelreuteria* (Sapindaceae) fruit, XTBGJL5-0029. (C) Unknown fruit with short petiole and a long branch, XTBGJL5-0028. (D) *Cedrelospermum* (Ulmaceae) fruit, XTBGJL5-0033. (E) Unknown inflorescence, XTBGJL5-0331. (F) *Lagokarpos tibetensis* (unknown family), XTBGJL5-0802 (1). (G) *Illigera* (Hernandiaceae) fruit, XTBGJL5-0512. (H) *Limnobiophyllum* (Araceae) whole plant, XTBGJL5-0177. (I) Legume (Fabaceae) fruit 3, XTBGJL5-0464. (J) cf. *Colocasia* (Araceae) tubers, XTBGJL5-0231. (K) Unknown fruit with long pedicel, XTBGJL5-0318. (L) Cedreleae (Meliaceae) seed, XTBGJL5-0034. (M) *Ceratophyllum* (Ceratophyllaceae) fruit, XTBGJL5-0545. (N) *Asclepiadospermum ellipticum* (Apocynaceae), XTBGJL5-0459 (3). (O) *Stephania* (Menispermaceae) endocarp, XTBGJL5-0524. (P) *Asclepiadospermum marginatum* (Apocynaceae) seed, XTBGJL5-0432 (3). (Q) Unknown winged fruit, XTBGJL5-0214. Scale bar = 1 cm.



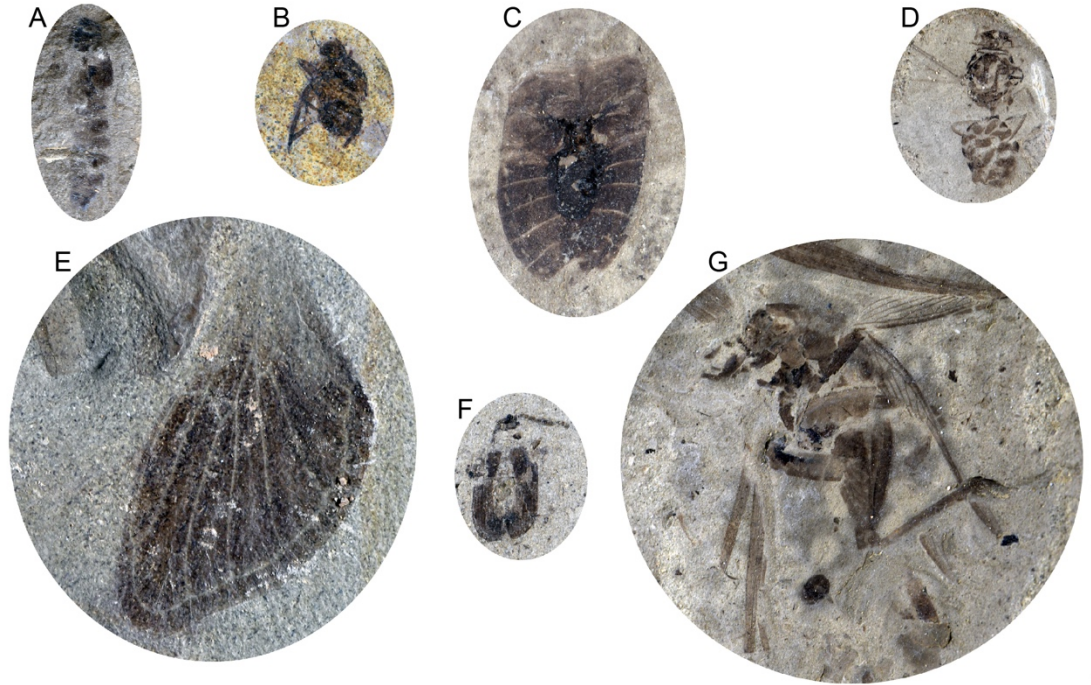
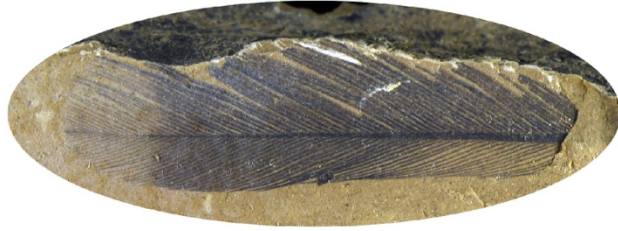


**Fig. S9.** Insect fossils associated with the Jiangliang flora, Bangor County, central Tibetan Plateau. (A) XZBGJL1-0076. (B) XZBGJL1-417. (C) XZBGJL5-0064. (D) XZBGJL5-0073. (E) XZBGJL5-0075. (F) XZBGJL5-0298. (G) XZBGJL5-0160. Scale bar = 1 cm.



A



B



C



**Fig. S10.** Feather and fish fossils collected from the same site in Jianglang, Bangor County, central Tibetan Plateau. (A) IVPP V26566. (B) IVPP V26565. (C) IVPP V26564. Scale bar = 1 cm.

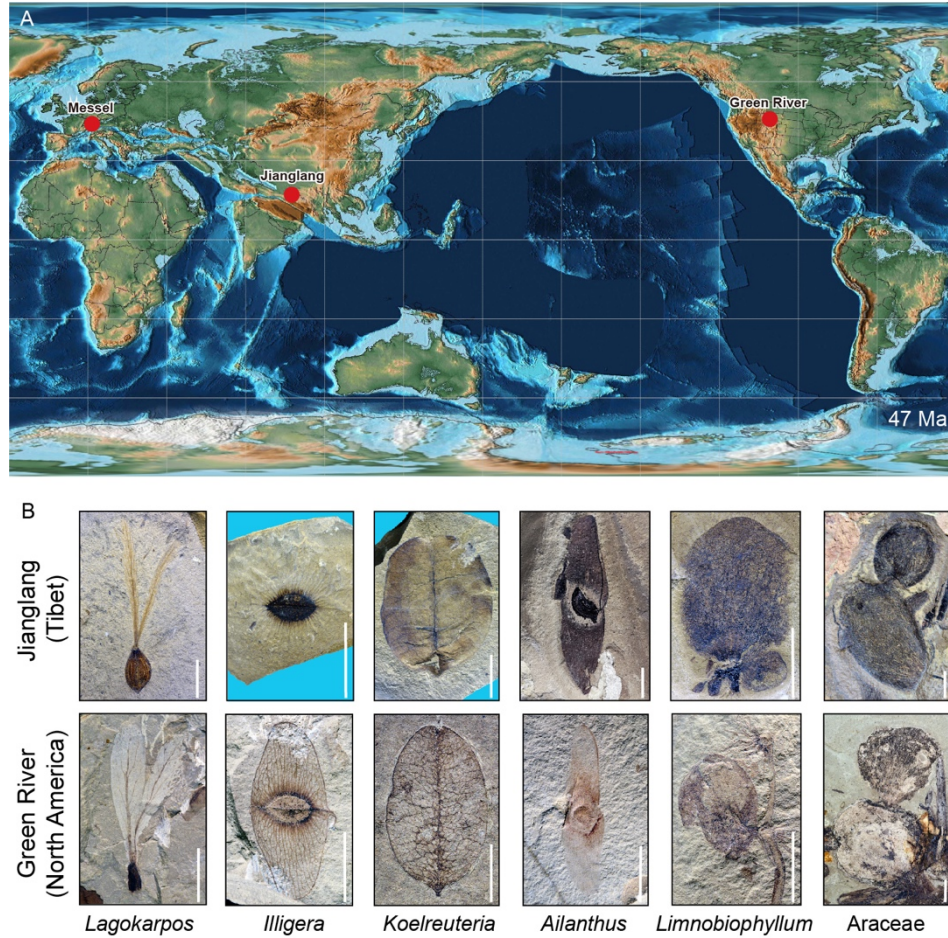


**Fig. S11.** Distribution of three middle Eocene floras in the Northern Hemisphere and their floristic similarity. (A) Spatial distributions of Jianglang, Green River, and Messel at ~47 Ma, map is modified after the PALEOMAP Project (<http://www.scotese.com>). (B) Fossil taxa from Jianglang flora and Green River flora indicate the close floristic similarity. Scale bar = 1 cm.

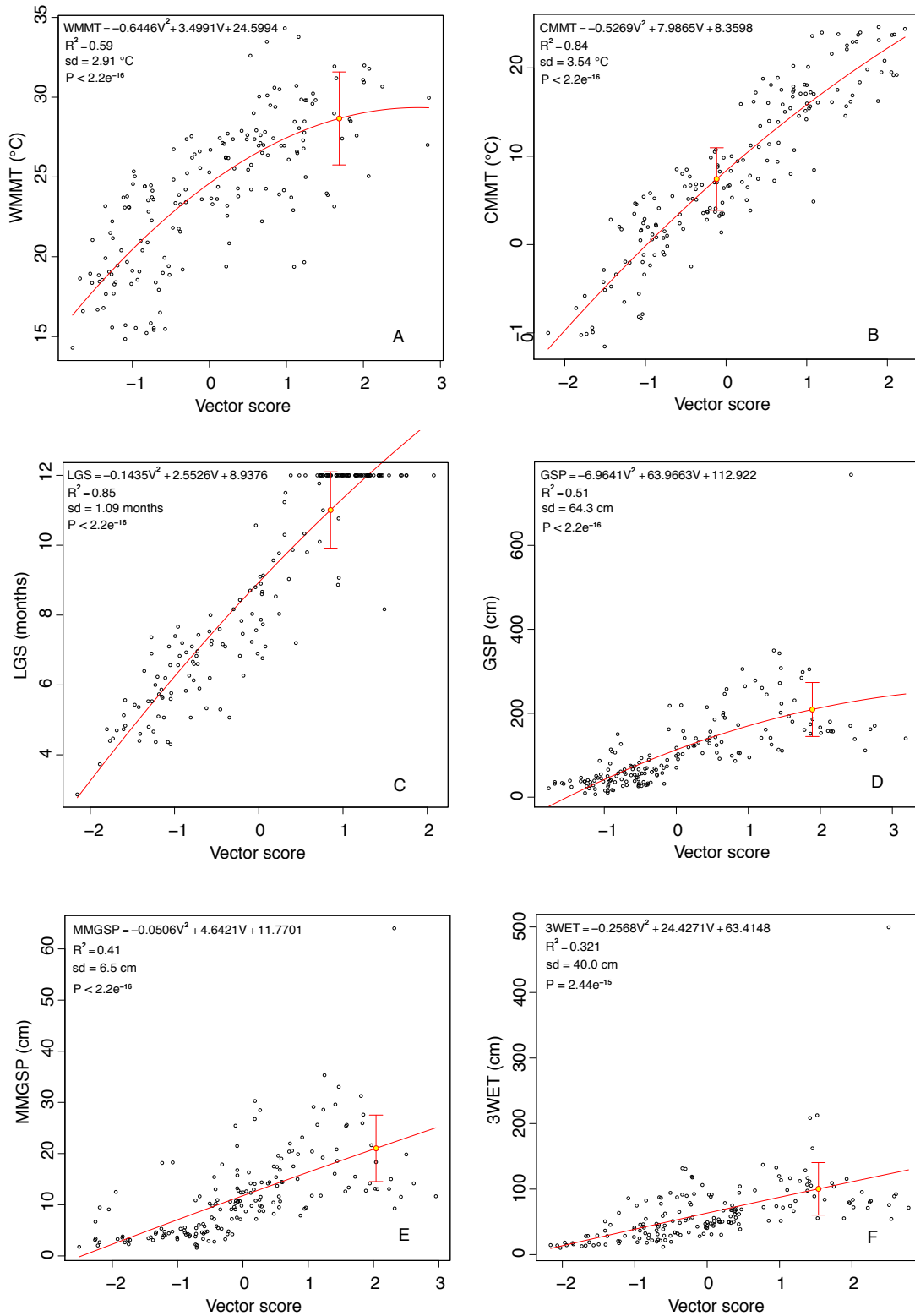


**Fig. S12.** Climate-Leaf Analysis Multivariate Program (CLAMP) vector score (V) and observed climate regressions. Calibration using the PhysgAsia2 leaf physiognomy dataset (*SI Appendix*, Table S4) paired with the WorldClim2\_GridMet\_Asia2AZ\_24var climate data (*SI Appendix*, Table S5). Black open circles represent the modern calibration data points, yellow filled red circle is



predicted position of the Jianglang flora, bars represent  $\pm 1$  s.d. (A) warm month mean air temperature (WMMT), (B) cold month mean air temperature (CMMT), (C) length of the growing season (LGS), (D) growing season precipitation (GSP), (E) mean monthly growing season precipitation (MMGSP), (F) precipitation in the three consecutive wettest months (3WET).

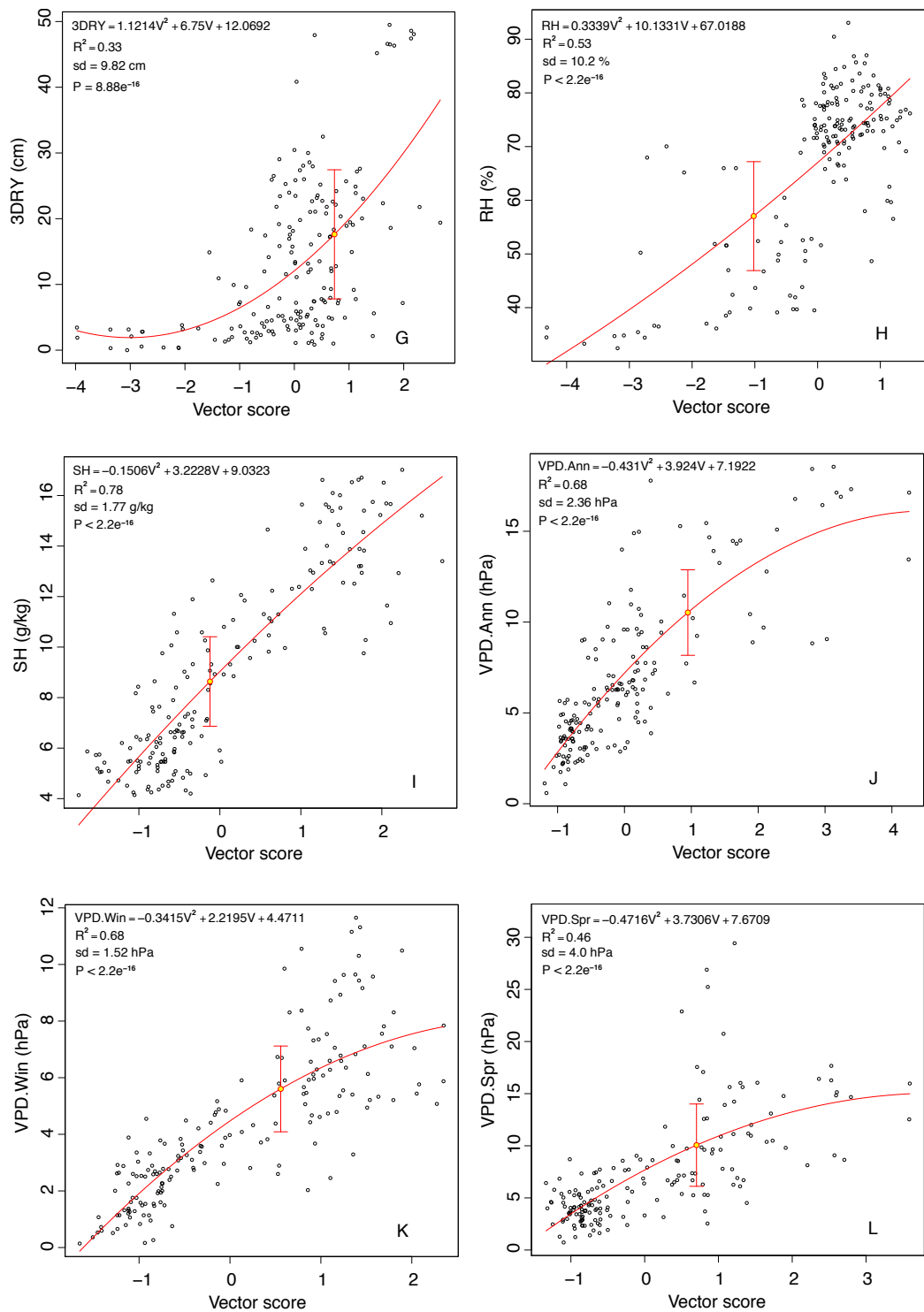


**Fig. S13.** Climate-Leaf Analysis Multivariate Program (CLAMP) regressions. (Continued 2). (G) precipitation in the three consecutive driest months (3DRY), (H) mean annual relative humidity (RH), (I) mean annual specific humidity (SH), (J) mean annual vapor pressure deficit (VPD.Ann), (K) mean vapor pressure deficit during winter (DJF) (VPD.Win), (L) mean vapor pressure deficit during spring (MAM) (VPD.Spr).

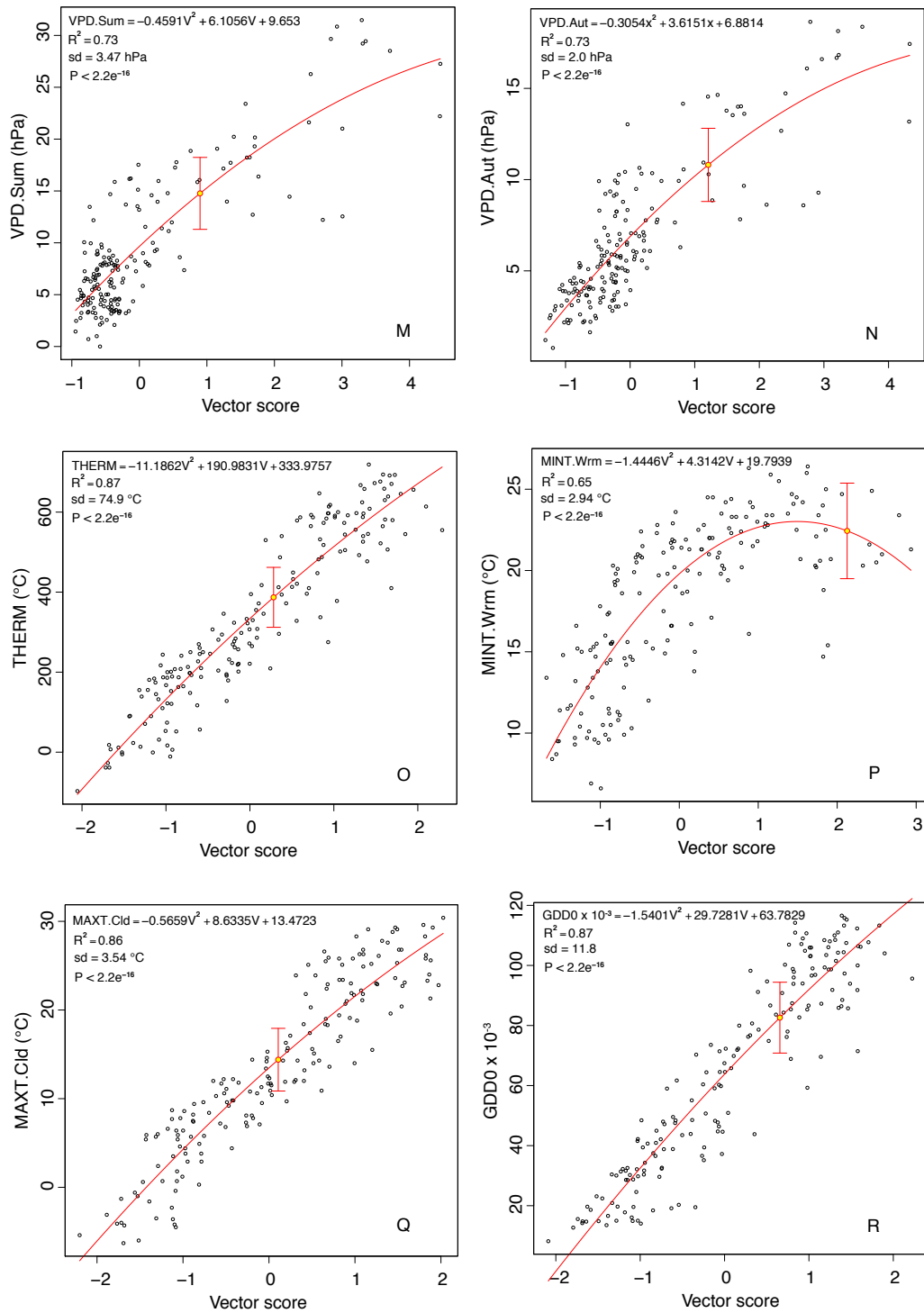


**Fig. S14.** Climate-Leaf Analysis Multivariate Program (CLAMP) regressions. (Continued 3). (M) mean vapor pressure deficit during summer (JJA) (VPD.Sum), (N) mean vapor pressure deficit during fall (SON) (VPD.Aut), (O) mean annual thermicity (THERM), (P) mean minimum temperature of the warmest month (MINT.Wrm), (Q) mean maximum temperature of the coldest month mean (MAXT.Cld), (R) growing degree days above 0°C (GDD0).



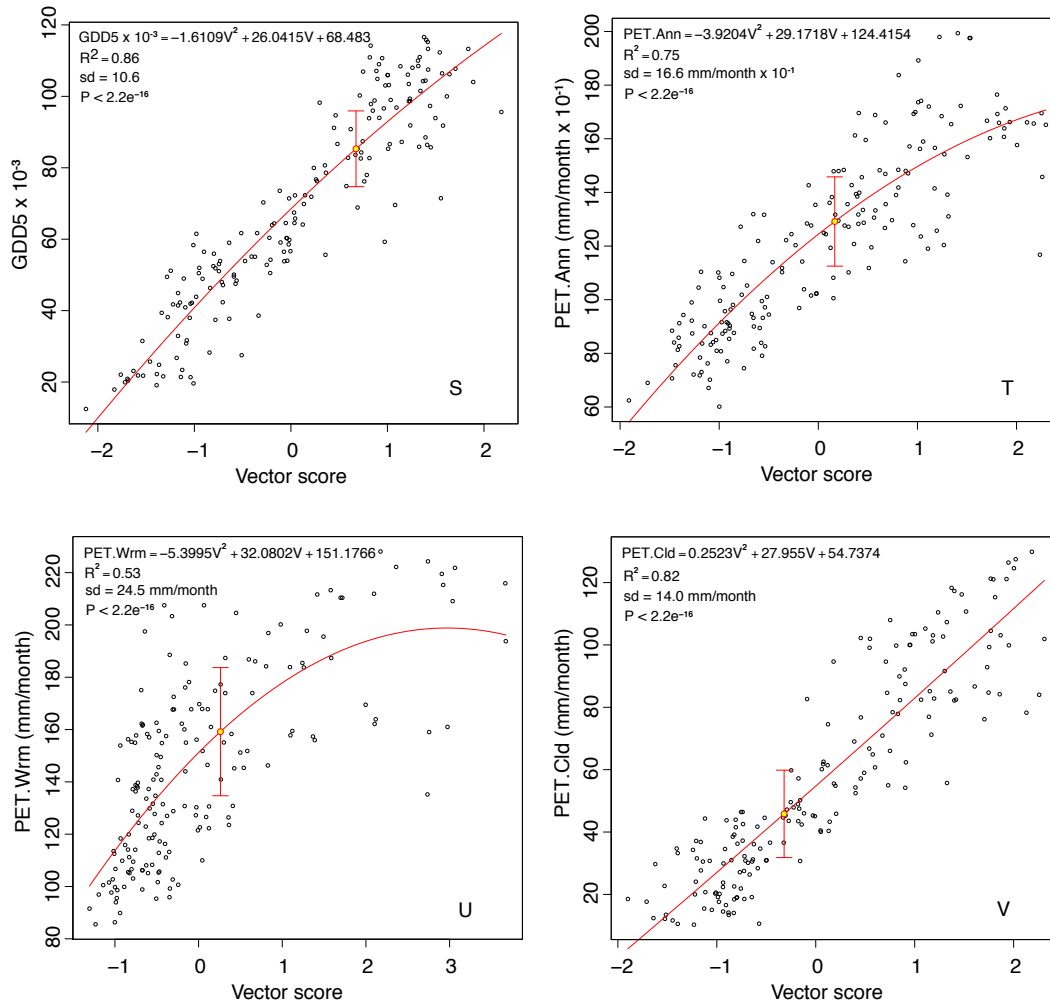


**Fig. S15.** Climate-Leaf Analysis Multivariate Program (CLAMP) regressions. (Continued 4). (S) growing degree days above 5 °C (GDD5), (T) mean annual potential evapotranspiration (PET.Ann), (U) mean evapotranspiration during the warmest month (PET.Wrm), (V) mean potential evapotranspiration during the coldest month (PET.Cld).

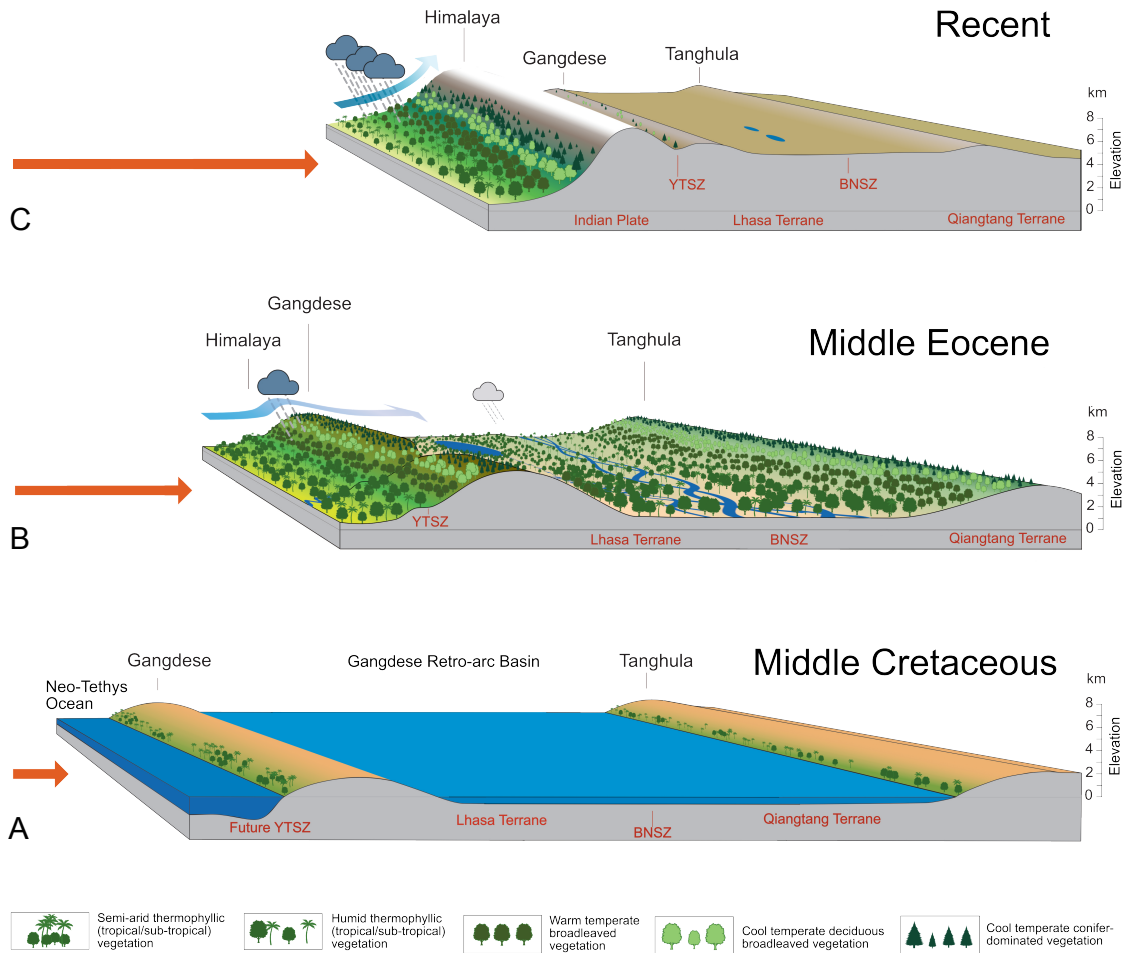


**Fig. S16.** Cartoons showing the evolution of the Himalaya and Tibet from the Middle Cretaceous to present (modified from (4)). (A) Middle Cretaceous (~110 Ma) with aridity-adapted vegetation restricted to coastal regions and lowlands where the groundwater is near the soil surface. What will later become the central Tibetan valley is shallow marine, occupying the Gangdese Retro-arc Basin and accommodating the remnants of the old Meso-Tethys Ocean (5). The monsoon is weak to non-existent (6) and the landscape is generally arid. (B) Middle Eocene (~45Ma) showing a deep valley between the Gangdese and Tanghula uplifts. Although the elevation history of the Tanghula is poorly quantified, the eastern Tanghula had achieved near modern elevations by the middle Eocene (7). As evidenced by the Niubao Formation sediments, within the valley fluvial deposition predominates and at least one river transects the Gangdese southwards (8) affording limited biotic connection with India. The climate is weakly monsoonal (indicated by a single cloud) but moisture is able to pass over the Gangdese highland to supply the subtropical vegetation in the Banggong-Nujiang suture zone (BNSZ) valley system. The Himalaya are beginning to rise south of the Yarlung-Tsangpo suture zone (YTSZ). (C) The Himalaya and Tibet today with a strong monsoon, but moisture largely blocked from the high, cold plateau by the Himalaya, resulting in a generally arid landscape. Red arrow represents relative movement driven by the India-Eurasia collision. Horizontal dimension not to scale.

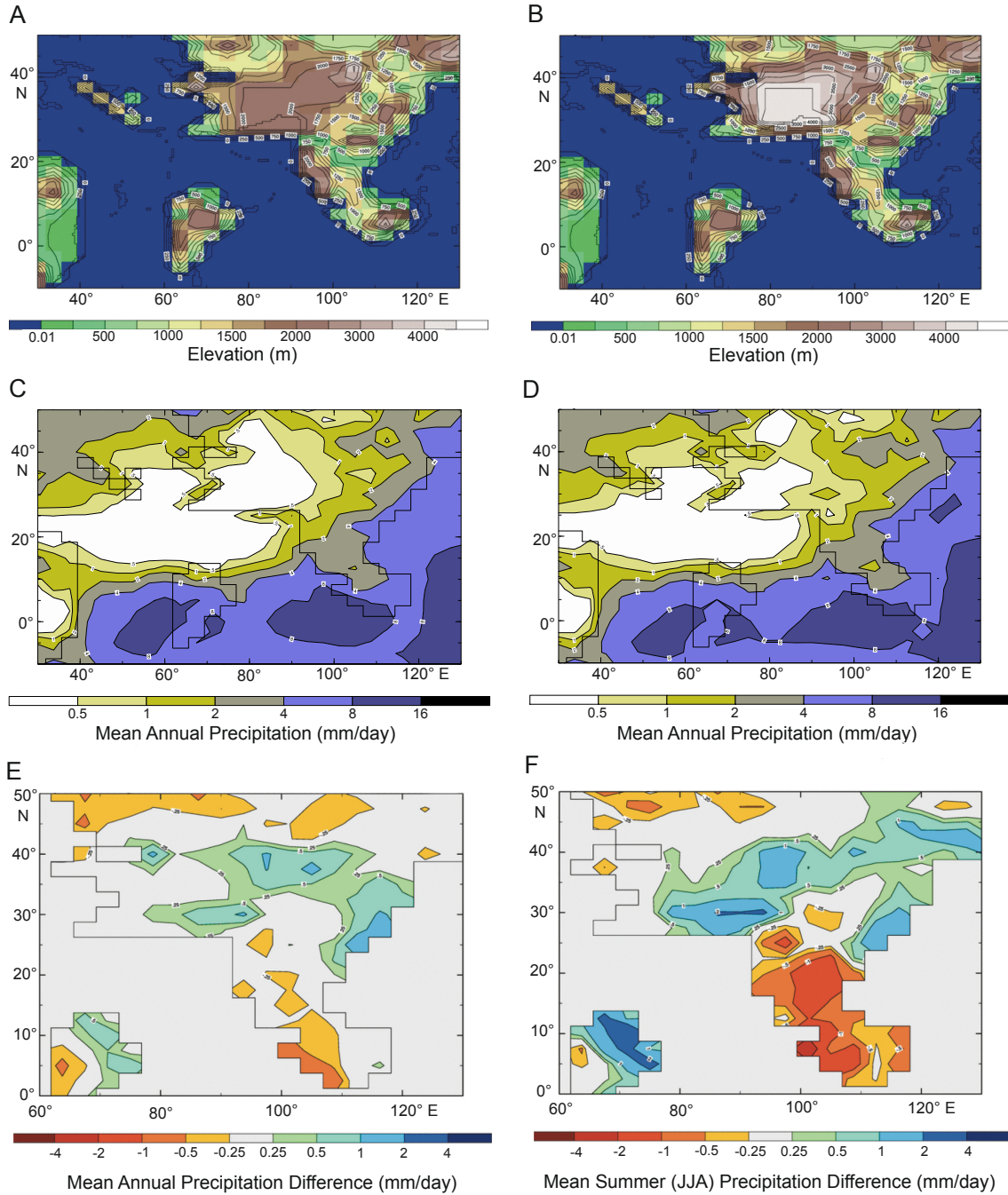


**Fig. S17.** Two climate model sensitivity studies for the Lutetian (~44 Ma) where the Tibetan Plateau is set at a 2 km elevation (A) and the same experiment where the Tibetan Plateau has been raised to 4 km elevation (B). The annual precipitation (mm/day) response for the 2 km (C) and 4 km (D) Tibetan Plateau is shown, with the difference in precipitation (mm/day) from changing Tibetan plateau height (4 km minus 2 km Tibetan Plateau) as an annualized (E) and June-August (F) response. The precipitation on the plateau itself is reduced only slightly as the plateau is raised, but the effects off the plateau are greater.

Table S1. Result of U-Pb zircon dating from a tephra-rich horizon just below the fossil assemblage XZBGJL5.

Analyses	Content (ppm)				Isotopic ratio								Age (Ma)							
	Pb	Th	U	Th/U	<sup>207</sup> Pb/ <sup>206</sup> Pb	1σ	<sup>207</sup> Pb/ <sup>238</sup> U	1σ	<sup>206</sup> Pb/ <sup>238</sup> U	1σ	<sup>207</sup> Pb/ <sup>206</sup> Pb	1σ	<sup>207</sup> Pb/ <sup>235</sup> U	1σ	<sup>206</sup> Pb/ <sup>238</sup> U	1σ				
JL-1-01	38.2	218.8	430.6	0.51	0.0495	0.0011	0.1327	0.0052	0.0195	0.0007	172.3	50.0	126.5	4.7	124.2	4.3				
JL-1-02	175.4	254.8	219.7	1.16	0.0573	0.0010	0.6645	0.0167	0.0841	0.0017	501.9	33.3	517.3	10.3	520.6	10.0				
JL-1-03	54.0	339.2	602.0	0.56	0.0485	0.0010	0.1211	0.0028	0.0181	0.0003	124.2	50.0	116.1	2.6	115.6	1.8				
JL-1-04	138.8	270.8	2183.6	0.12	0.0864	0.0028	0.1854	0.0039	0.0157	0.0007	1347.2	61.1	172.7	3.4	100.4	4.4				
JL-1-05	143.6	194.1	237.5	0.82	0.0591	0.0012	0.7130	0.0155	0.0876	0.0016	572.3	30.5	546.5	9.3	541.1	9.8				
JL-1-06	134.0	75.3	214.1	0.35	0.0752	0.0010	1.9287	0.0434	0.1860	0.0040	1073.8	27.8	1091.1	15.2	1099.7	21.9				
JL-1-07	127.1	729.8	860.7	0.85	0.0511	0.0014	0.1387	0.0033	0.0197	0.0005	255.6	47.2	131.9	3.0	126.0	3.4				
JL-1-08	74.6	302.3	332.1	0.91	0.0516	0.0016	0.1885	0.0057	0.0266	0.0008	333.4	86.1	175.3	4.8	169.1	5.1				
JL-1-09	78.8	351.5	397.4	0.88	0.0860	0.0034	0.2181	0.0100	0.0184	0.0003	1338.9	63.9	200.4	8.3	117.4	2.1				
JL-1-10	76.3	1143.1	1077.6	1.06	0.0502	0.0018	0.0519	0.0016	0.0075	0.0002	205.6	88.9	51.3	1.6	48.2	1.3				
JL-1-11	215.1	209.8	71.9	2.92	0.0667	0.0016	1.0954	0.0358	0.1190	0.0027	827.8	63.9	751.1	17.4	724.9	15.5				
JL-1-12	28.5	140.5	259.5	0.54	0.0537	0.0025	0.1451	0.0060	0.0197	0.0005	366.7	105.5	137.6	5.3	125.5	3.4				
JL-1-13	36.3	200.7	282.8	0.76	0.0541	0.0027	0.1389	0.0058	0.0187	0.0005	372.3	97.2	132.1	5.2	119.5	3.2				
JL-1-14	33.0	129.8	206.9	0.63	0.0538	0.0026	0.1936	0.0086	0.0261	0.0004	364.9	105.5	179.7	7.4	166.2	2.7				
JL-1-15	20.4	57.9	75.8	0.76	0.2338	0.0107	0.4173	0.0277	0.1259	0.0005	3078.7	73.1	354.1	19.9	82.5	3.1				
JL-1-16	45.1	260.0	259.0	1.00	0.0524	0.0024	0.1324	0.0052	0.0183	0.0004	305.6	8.3	126.2	4.7	117.2	2.3				
JL-1-17	26.2	147.0	142.6	1.03	0.0583	0.0043	0.1480	0.0098	0.0185	0.0004	542.6	161.1	140.1	8.7	118.0	2.8				
JL-1-18	16.7	89.0	131.3	0.68	0.0563	0.0039	0.1421	0.0092	0.0184	0.0004	464.9	163.9	134.9	8.2	117.4	2.7				
JL-1-19	16.5	87.8	126.4	0.69	0.0576	0.0038	0.1461	0.0094	0.0184	0.0004	522.3	144.4	138.5	8.3	117.8	2.3				
JL-1-20	145.1	114.3	154.5	0.74	0.0694	0.0015	1.3470	0.0352	0.1409	0.0036	909.3	44.4	866.3	15.3	850.0	20.2				
JL-1-21	28.4	223.4	409.1	0.55	0.0544	0.0028	0.0922	0.0043	0.0124	0.0004	387.1	130.5	89.6	4.0	79.1	2.3				
JL-1-22	34.4	44.3	86.4	0.51	0.0591	0.0017	0.6850	0.0241	0.0816	0.0022	572.3	66.7	517.7	14.7	505.5	13.2				
JL-1-23	62.6	161.9	287.5	0.56	0.0533	0.0014	0.3021	0.0091	0.0412	0.0013	342.7	55.6	288.0	7.1	280.0	8.1				
JL-1-24	32.7	158.3	548.4	0.29	0.0515	0.0016	0.1331	0.0042	0.0188	0.0006	261.2	72.2	126.8	3.8	120.0	3.7				
JL-1-25	212.1	345.6	391.0	0.88	0.0565	0.0010	0.5410	0.0118	0.0694	0.0014	472.3	38.9	439.1	7.8	432.5	8.3				
JL-1-26	21.2	103.8	122.0	0.85	0.0656	0.0045	0.1717	0.0116	0.0190	0.0004	792.3	142.1	160.9	10.1	121.3	2.5				
JL-1-27	70.2	231.1	227.9	1.01	0.0529	0.0018	0.2444	0.0080	0.0335	0.0006	324.1	77.8	222.0	6.5	212.4	4.0				
JL-1-28	126.3	79.5	50.7	1.57	0.0815	0.0023	2.0615	0.0805	0.1832	0.0041	1233.0	56.5	1136.1	26.8	1084.2	22.7				
JL-1-29	139.8	401.8	594.0	0.68	0.0527	0.0011	0.2477	0.0145	0.0341	0.0019	322.3	50.0	224.7	11.8	216.0	12.0				
JL-1-30	44.2	234.9	281.1	0.84	0.0643	0.0038	0.1595	0.0086	0.0180	0.0003	750.0	122.2	150.2	7.6	115.2	2.2				
JL-1-31	224.2	165.8	459.0	0.36	0.0673	0.0011	1.2079	0.0448	0.1300	0.0046	850.0	36.6	804.2	20.7	787.7	26.5				
JL-1-32	51.3	118.3	167.0	0.71	0.0547	0.0021	0.3293	0.0113	0.0437	0.0009	398.2	83.3	289.0	8.6	275.8	5.5				
JL-1-33	258.8	710.1	396.0	1.79	0.0537	0.0013	0.3095	0.0070	0.0418	0.0008	366.7	50.0	273.8	5.5	264.0	4.9				
JL-1-34	78.9	223.5	218.0	1.03	0.0545	0.0019	0.2863	0.0073	0.0382	0.0009	390.8	77.8	255.6	5.8	241.8	5.3				
JL-1-35	291.8	448.9	586.5	0.77	0.0559	0.0009	0.5513	0.0119	0.0715	0.0017	450.0	33.3	445.8	7.9	445.1	10.4				
JL-1-36	180.1	129.3	118.7	1.09	0.0717	0.0013	1.5697	0.0294	0.1587	0.0022	988.9	37.5	958.3	11.8	949.3	12.6				
JL-1-37	162.7	406.5	445.5	0.91	0.0542	0.0012	0.3251	0.0070	0.0435	0.0007	376.0	50.0	285.8	5.4	274.7	4.2				
JL-1-38	12.7	45.6	298.0	6.81	0.0585	0.0033	0.7160	0.0830	0.0850	0.0077	610.0	120.0	547.0	53.0	533.0	45.0				
JL-1-39	111.8	1780.0	1380.0	0.84	0.0623	0.0034	0.1900	0.0110	0.0215	0.0015	670.0	110.0	175.9	9.1	137.4	9.2				
JL-1-40	31.3	304.0	1020.0	4.09	0.0508	0.0025	0.2840	0.0160	0.0388	0.0016	210.0	110.0	237.0	13.0	245.4	9.8				
JL-1-41	697.0	561.0	89.8	0.16	0.1636	0.0056	10.9600	0.3400	0.4768	0.0075	2483.0	56.0	2516.0	29.0	2513.0	33.0				
JL-1-42	101.9	181.0	158.4	0.91	0.0810	0.0029	2.2520	0.0930	0.2032	0.0054	1208.0	70.0	1200.0	27.0	1192.0	29.0				
JL-1-43	122.1	232.0	364.0	1.61	0.0807	0.0026	2.1160	0.0720	0.1848	0.0030	1152.0	64.0	1152.0	23.0	1093.0	17.0				
JL-1-44	163.0	689.0	1620.0	2.45	0.0585	0.0022	0.6740	0.0230	0.0811	0.0018	561.0	84.0	523.0	14.0	503.0	11.0				
JL-1-45	41.9	446.0	837.0	1.92	0.0578	0.0036	0.2280	0.0130	0.0286	0.0006	500.0	140.0	208.0	10.0	181.6	3.6				
JL-1-46	27.6	100.0	107.0	1.31	0.0633	0.0049	0.8670	0.0680	0.0976	0.0024	690.0	180.0	629.0	37.0	600.0	14.0				
JL-1-47	14.5	114.0	1280.0	11.43	0.0727	0.0052	0.1880	0.0120	0.0163	0.0004	950.0	150.0	158.0	11.0	104.3	2.2				
JL-1-48	136.7	318.0	549.0	1.82	0.0778	0.0023	1.6510	0.0480	0.1534	0.0026	1144.0	60.0	998.0	19.0	920.0	15.0				
JL-1-49	25.1	135.0	313.0	2.44	0.0656	0.0043	0.6090	0.0370	0.0651	0.0013	830.0	150.0	486.0	25.0	406.3	7.6				
JL-1-50	81.0	530.0	1880.0	4.32	0.0665	0.0025	0.3160	0.0310	0.0338	0.0029	833.0	79.0	277.0	24.0	214.0	18.0				
JL-1-51	32.6	63.8	760.0	12.60	0.0901	0.0031	2.2800	0.1700	0.1820	0.0110	1416.0	66.0	1201.0	56.0	1086.0	62.0				
JL-1-52	26.1	226.0	2180.0	11.10	0.0612	0.0024	0.2030	0.0190	0.0240	0.0024	646.0	81.0	187.0	16.0	153.0	15.0				
JL-1-53	46.9	200.0	239.0	1.31	0.0672	0.0041	0.7750	0.0440	0.0815	0.0017	860.0	140.0	580.0	25.0	505.2	9.8				
JL-1-54	92.0	189.0	818.0	4.74	0.1194	0.0032	2.7600	0.3300	0.1700	0.0200	1941.0	48.0	1328.0	91.0	1000.0	110.0				
JL-1-55	20.5	157.0	591.0	4.18	0.0563	0.0033	0.3220	0.0170	0.0412	0.0009	480.0	120.0	283.0	13.0	260.1	5.5				
JL-1-56	17.2	773.0	1300.0	1.70	0.0477	0.0043	0.0496	0.0042	0.0073	0.0002	100.0	49.1	4.0	46.7	1.1	1.1				
JL-1-57	50.7	2500.0	1720.0	0.73	0.0450	0.0040	0.0466	0.0041	0.0073	0.0002	-20.0	180.0	46.1	4.0	46.9	1.3				
JL-1-58	10.2	216.0	347.0	1.64	0.0553	0.0085	0.1060	0.0170	0.0136	0.0006	330.0	330.0	101.0	15.0	87.1	3.8				
JL-1-59	22.9	504.0	682.0	1.57	0.0493	0.0044	0.1120	0.0110	0.0167	0.0004	160.0	200.0	107.5	9.9	106.7	2.7				
JL-1-60	66.5	302.0	159.0	0.55	0.0576	0.0059	0.6300	0.0650	0.0781	0.0024	490.0	230.0	490.0	40.0	485.0	15.0				
JL-1-61	109.3	121.2	306.0	2.69	0.1168	0.0020	5.4500	0.1100	0.3315	0.0064	1891.0	32.0	1851.0	17.0	1851.0	30.0				
JL-1-62	32.8	142.0	3410.0	24.47	0.0717	0.0014	0.6500	0.0290	0.0648	0.0026	982.0	42.0	507.0	18.0	405.0	16.0				
JL-1-63	10.3	94.0	503.0	5.78	0.0516	0.0043	0.2880	0.0230	0.0374	0.0008	220.0	170.0	240.0	18.0	236.5	5.0				
JL-1-64	62.8	81.2	172.6	2.10	0.1064	0.0033	4.3300	0.1400	0.2930	0.0064	1740.0	60.0	1695.0	28.0	1656.0	32.0				
JL-1-65	24.1	136.9	214.0	1.55	0.0545	0.0043	0.4510	0.0340	0.0602	0.0014	410.0	190.0	376.0	24.0	376.9	8.7				
JL-1-66	67.6	261.0	328.2	1.55	0.0650	0.0034	0.7870	0.0380	0.0875	0.0018	770.0	110.0	588.0	21.0	540.0	11.0				
JL-1-67	38.0	101.0	289.0	5.00	0.0674	0.0029	1.2450	0.0530	0.1340	0.0021	852.0	82.0	825.0	22.0	811.0	12.0				
JL-1-68	351.0	361.0	227.0	0.65	0.1453	0.0034	8.1800	0.2000	0.4130	0.0110	2286.0									



**Table S2.** Floristic components of the Jiangling flora, central Tibetan Plateau, and the floristic comparison to Green River flora in western interior USA, and Messel flora in Germany.

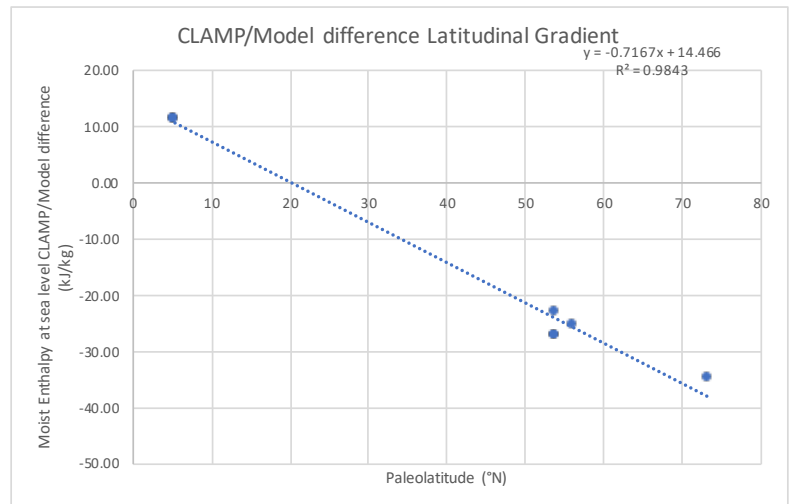
No.	Species	Specimens checked	Figure No.	Key characters for classification	Major distribution of modern relatives	Green River flora	Messel flora
1	<i>Ailanthus maximus</i> (Simaroubaceae) samara	XZBGJL1-0009, XZBGJL5-0007	Figure S4, O; Figure S8, A	Samara large, about 60 mm long. Main ventral vein located in the intramarginal part of the samara. The stylar scar at the same level as the middle of the seed.	Temperate, subtropical, tropical	<i>Ailanthus confucii</i>	<i>Ailanthus confucii</i>
2	<i>Asclepiadospermum ellipticum</i> (Apocynaceae) seed	XZBGJL2-0009, XZBGJL5-0459	Figure S5, A; Figure S8, N	Seed elliptic, tapering rapidly toward a blunt to slightly rounded and asymmetrical apex and rounded at the base. Central part elliptical and irregularly spotted, surrounded by a thin margin with a straight median line corresponding to the trace left by the raphe from the apex to the center of the seed. Cells small (~30 µm wide), polygonal, and irregularly arranged.	Subtropical, tropical		
3	<i>Asclepiadospermum marginatum</i> (Apocynaceae) seed	XZBGJL5-0432	Figure S8, P	Seed pear-shaped, tapering rapidly toward a blunt to slightly rounded apex with a small bump, and rounded at the base; central part oval and smooth, surrounded by a wide margin. A straight median line corresponding to the trace left by the raphe from the apex to the center of the seed. Cells polygonal and winged samara-like seed, 8 mm length, locule body proximal and elliptical enclosing a round embryo. One wing laterally striated and bordered by a strong marginal vein in one side.	Subtropical, tropical		
4	<i>Cedrelae</i> (Meliaceae) winged seed	XZBGJL5-0034	Figure S8, L		Subtropical, tropical		
5	<i>Cedrelopspermum</i> (Ulmaceae) fruit	XZBGJL5-0033	Figure S8, D	Stem supporting 5 alternate young fruits with a small pedicel. Fruits winged (decayed) with an elliptical fruit body, ~8 mm in length, ~4 mm in width.		<i>Cedrelopspermum nervosum</i>	<i>Cedrelopspermum leptospermum</i>
6	<i>Ceratophyllum</i> (Ceratophyllaceae) achene	XZBGJL5-0545	Figure S8, M	Achene ellipsoidal, surface of the body smooth, possibly warty, length 3.0 mm, width 2.2 mm (LW ratio=1.4). Body surrounded by 11 lateral spines, 0.5–1.7 mm in length. Presence of a stylar spine slightly eccentric and two paired basal spines.	Temperate, subtropical, tropical	<i>Ceratophyllum muricatum</i>	
7	<i>cf. Pachysandra</i> (Buxaceae) fruit	XZBGJL4-0003	Figure S5, O	Stem supporting several fruits (capsule) ovoid and longitudinally striated, 15 mm long, 7 mm width, with 3 stylar appendages, ca. 1 cm long each.	Temperate, subtropical		Buxaceae
8	<i>Illigera</i> (Hernandiaceae) fruit	XZBGJL1-0005, XZBGJL1-0004, XZBGJL1-0005, XZBGJL1-0006, XZBGJL5-0512	Figure S4, A; Figure S8, G	Fruit with a locule shape fusiform, bisected by a median ridge in the plane of bisymmetry. Veins fanning outward radially. Wing shape orbicular or suborbicular. Height 6–8 mm, width 2–5 mm.	Tropical	<i>Illigera eocenica</i>	
9	<i>Koeleruteria</i> (Sapindaceae) capsular valves	XZBGJL5-0029, XZBGJL5-0381, XZBGJL5-0511	Figure S8, B	Capsular valves slightly asymmetrical, elliptical to orbicular in outline. Apex emarginate, base acuminate, lateral veins irregularly zigzag forming a random reticulation. Length ca. 33 mm, width ca. 27 mm.	Temperate, subtropical, tropical	<i>Koeleruteria allenii</i>	
10	<i>Lagokarpus tibetensis</i> (unknown family) fruit	XZBGJL1-0383, XZBGJL5-0802	Figure S4, F; Figure S8, F	Fruit consisting of two elongate V patterned wings arising from the apex of an elliptical fruit body. Wings entire-margined and pinnate venation patterned.		<i>Lagokarpus lacustris</i>	<i>Lagokarpus</i> sp.
11	Legume (Fabaceae) fruit 1	XZBGJL1-0012	Figure S4, B	Pod incomplete, 4–8 mm in length with an acute apex, margin thin ca. 0.5 mm, seeds number at least 3, round, ca. 3 mm in diameter.	Temperate, subtropical, tropical	Legume (Fabaceae) fruit	Legume (Fabaceae) fruit
12	Legume (Fabaceae) fruit 2	XZBGJL3-0009	Figure S5, M	Pod incomplete, at least 4.3 mm length, 3.4 mm width crossed by a median line corresponding to the vasculature, constricted following each internal seeds, seed number at least 8, oval, ca. 4 mm in length.	Temperate, subtropical, tropical		
13	Legume (Fabaceae) fruit 3	XZBGJL5-0464	Figure S8, K	Pod incomplete, at least 18 mm length, 1.8 mm width, constricted following each internal seeds, apex truncated, margin thin, ca. 0.2 mm, seed number at least 6, oval, ca. 2.4 mm in length.	Temperate, subtropical, tropical		
14	<i>Passiflora</i> (Passifloraceae) seed	XZBGJL1-0007, XZBGJL5-0255	Figure S4, D	Seed compressed, ovoid to elliptic, apex rounded to slightly acute, base rounded, surface of the seed densely covered by round pits randomly arranged. Length and width less than 10 mm.	Tropical		
15	<i>Stephania</i> (Menispermaceae) endocarp	XZBGJL1-0021, XZBGJL1-0009, XZBGJL5-0056, XZBGJL5-0057, XZBGJL5-0141, XZBGJL5-0524	Figure S4, C; Figure S5, N; Figure S8, O	Endocarp horsehoe-shaped, dorsal crest apparently smooth; lateral face with a small elliptical and excavated central area surrounded by a horsehoe-like lateral crest; dorsal part of the lateral crest connected to the dorsal crest by ca. 10–12 transverse and spiny ribs. A straight-vascular tube run to the base of the condyle area up to center of the endocarp.	Subtropical, tropical	<i>Stephania wilii</i>	<i>Stephania hootei</i>
16	Vitaceae endocarp	XZBGJL1-0018, XZBGJL1-0035	Figure S4, I	Endocarp horsehoe-shaped, lateral face with a broad elliptical and excavated central area surrounded by a horsehoe-like lateral crest; dorsal part of the lateral crest connected to the dorsal crest by ca. 13 to 15 small, transverse and rectangular ribs. Limits of the locule cast unequal length at the base, ventral notch slightly asymmetrical, straight vascular tube running to the base of the condyle area up to center of the endocarp.	Temperate, subtropical, tropical	<i>Ampelocissus auriforma</i>	Vitaceae seed
17	Seed cordiform with a prominent ridge (unknown)	XZBGJL1-0019, XZBGJL1-0020, XZBGJL5-0187	Figure S4, G	Seed cordiform, apex emarginate, paired of ventral infold centered, slightly curved and diverging apically. Chalazae elongate connected with the raphe by a prominent ridge. Length of the seed 4–5 mm.			<i>Carpollithus</i> sp.
18	Winged fruit with radial veins (unknown)	XZBGJL1-0033, XZBGJL5-0214, XZBGJL5-0347	Figure S4, L; Figure S8, Q	Winged fruit, 22–25 mm length, 9–11 mm width, seed centered and round surrounded by two or more wings, with 11–13 lateral venation spanning from the seed and fusing with the marginal venation, thick pedicel at the base.			
19	Unknown oblong fruit with pedicels	XZBGJL1-0022	Figure S4, N	Fruit oblong, 17 mm length, 5 mm width, short sepals almost cupulate present at the base, at least 5.			
20	Unknown obovate fruit	XZBGJL1-0010	Figure S4, E	Fruit obovate with a petiole, 8–11 mm length, 5–7 mm width, margin thick, ca. 0.6 mm, body finely pitted or dotted.			
21	Fruit oblong and slender pedicel	XZBGJL3-0011	Figure S5, J	Fruit oblong, 6 mm length, 2 mm width. Pedicel slender, 3 mm in length.			
22	Fruit with long pedicel (unknown)	XZBGJL5-0318	Figure S8, K	Fruit 10 mm length, with a body of ca. 5 mm length and 3 mm long and a pedicel of ca. 6 mm.			
23	Fruit with short pedicel attaching to a stem (unknown)	XZBGJL5-0028	Figure S8, C	Stem supporting a fruit with a short pedicel, fruit ca. 16 mm length, ca. 6 mm width.			
24	Fruit or seed with ridges (unknown)	XZBGJL3-0013	Figure S5, G	Fruit or seed, ca. 5 mm length, ca. 2 mm width, with two longitudinal ridges spreading from the base to the apex.			
25	Flower (unknown)	XZBGJL1-0008	Figure S4, K	Flower single with a pedicel 7 mm in length. Petals elliptic with veins. Two blending stamens observed.			
26	Inflorescence (unknown)	XZBGJL5-0331	Figure S8, E	Inflorescence raceme, 25 mm in length, >13 flowers with pedicel ~0.5 mm in length.			
27	<i>cf. Colocasia</i> (Araceae) tuber	XZBGJL1-0011, XZBGJL1-0024, XZBGJL2-0001, XZBGJL5-0134, XZBGJL5-0141, XZBGJL5-0231, XZBGJL5-0465, XZBGJL5-0529, XZBGJL5-0531	Figure S4, J; Figure S5, B; Figure S8, J	Tubers ovoid to spherical, ~20–65 mm in length and ~10–40 mm in width. Buds on fibrous tuber surface.	Temperate, subtropical, tropical	<i>Carpollithus filiferus</i>	
28	<i>Limnophyllum</i> (Araceae) whole plant	XZBGJL5-0177	Figure S8, H	Plant with 1–2 widely ovate to orbicular leaves, inter-connected by stolon. Leaf entire, hairy, with an apical notch and numerous roots at the base. Leaf venation campydomous, secondary veins 10–14. Long petiole arising near leaf base. Inflorescence bearing about 40 seeds, surrounded by spathe. Seeds ellipsoid and ribbed.		<i>Limnophyllum acutum</i>	
29	<i>Cedrelopspermum</i> (Ulmaceae) leaf	XZBGJL1-0016, XZBGJL1-0030, XZBGJL3-0004, XZBGJL5-0356, XZBGJL5-0179, XZBGJL5-0410, XZBGJL5-0533	Figure S4, V; Figure S5, F; Figure S6, G	Leaf petiolate. Blade oblong, ~9–27 mm × 4–9 mm. Apex straight; Base rounded. Margin serrate. Secondary veins 8–10 pairs, craspedodromous, sometimes with bifurcation, 30–45° to midvein. Tertiary veins mixed percurrent.			
30	<i>Ailanthus</i> (Simaroubaceae) leaf	XZBGJL5-0388	Figure S7, N	Blade oblong, >76 mm × 29 mm. Base asymmetrical. Margin entire. Secondary veins >12 pairs, hemieucampodromous, 50–75° to midvein. Tertiary veins mixed percurrent. Higher-level veins irregular reticulate.	Temperate, subtropical, tropical		
31	<i>cf. Banksia</i> (Proteaceae) leaf	XZBGJL3-0002, XZBGJL5-0037, XZBGJL5-0143, XZBGJL5-0148, XZBGJL5-0236, XZBGJL5-0354, XZBGJL5-0382	Figure S5, D; Figure S6, A	Blade linear, ~53 mm × 3–5 mm. Margin serrate. Secondary veins >35 pairs, craspedodromous, 45–60° to midvein.	Tropical	<i>Banksia comptrofolia</i>	
32	<i>Cardiospermum</i> (Sapindaceae) leaf	XZBGJL1-0025, XZBGJL1-0026, XZBGJL1-0029, XZBGJL5-0348, XZBGJL5-0520	Figure S4, R; Figure S6, D	Leaf alternate pinnately compound with winged petiole. Leaflets sessile, ~16–20 mm × 4–6 mm. Apex straight. Base asymmetrical. Margin serrate.	Tropical	<i>Cardiospermum coloradensis</i>	
33	<i>cf. Comptonia</i> (Myricaceae) leaf	XZBGJL5-0250	Figure S6, C	Leaf alternate pinnately lobed. Blade linear, >15 mm × 4 mm. Apex convex. Secondary veins craspedodromous, 40–50° to midvein.	Temperate, subtropical	<i>Comptonia</i> sp.	
34	<i>cf. Lomaxia</i> (Proteaceae) leaf	XZBGJL1-0001, XZBGJL1-0039	Figure S4, H	Leaf obovate-pinnately lobed with 7 pairs of leaflets. Leaf petiolate. Blade ovate, ~110 mm × 24 mm. Apex straight. Secondary veins 7 pairs, craspedodromous, 30–40° to midvein.	Tropical	<i>Lomaxia lineata</i>	
35	Legume (Fabaceae) leaflet	XZBGJL5-0123	Figure S6, J	Leaf sessile. Blade lanceolate, ~13 mm × 3 mm. Base asymmetrical. Margin entire. Secondary veins pairs, brochidodromous, 45° to midvein.	Temperate, subtropical, tropical	<i>Parvilignumphyllum coloradensis</i>	
36	<i>Macclintockia</i> (unknown family) leaf	XZBGJL5-0245	Figure S6, H	Leaf petiolate. Blade, ~40 mm × 26 mm. Base decurrent. Margin crenate. Primary veins 5-acropodromous. Tertiary veins convex opposite percurrent.			
37	Menispermaceae leaf	XZBGJL3-0010, XZBGJL5-0195, XZBGJL5-0544	Figure S5, K; Figure S7, I	Leaf petiolate. Blade obovate, ~46–84 mm × 54–68 mm. Apex straight; Base cordate. Margin entire. Primary veins 7-acropodromous. Tertiary veins opposite percurrent.	Subtropical, tropical		
38	Myrtales leaf	XZBGJL5-0168, XZBGJL5-0339	Figure S6, L	Blade lanceolate, >55 mm × 11 mm. Base decurrent. Margin entire. Secondary veins ~12 pairs, brochidodromous, 45–55° to midvein. Interscedanaries prominent.	Subtropical, tropical		
39	Sapindaceae leaf	XZBGJL3-0001	Figure S5, C	Leaf sessile. Blade lanceolate, ~150 mm × 33 mm. Base asymmetrical. Margin serrate. Secondary veins 17 pairs, semicraspedodromous, 45–80° to midvein. Interscedanaries prominent. Tertiary veins opposite percurrent.	Temperate, subtropical, tropical		
40	<i>Syzygioides</i> (Myrtaceae) leaf	XZBGJL5-0292	Figure S6, O	Blade lanceolate, ~18 mm × 3 mm. Base decurrent. Margin entire. Secondary veins ~15 pairs, brochidodromous, forming intramarginal secondary, 45° to midvein. Interscedanaries prominent.	Subtropical, tropical	<i>Syzygioides americana</i>	
41	<i>Ziziphus</i> (Rhamnaceae) leaf	XZBGJL1-0023	Figure S4, T	Leaf petiolate. Blade ovate, ~30 mm × 17 mm. Apex acuminate; Base truncate. Margin crenate. Primary veins 3-acropodromous. Secondary veins 5 pairs, semicraspedodromous.	Temperate, subtropical, tropical		
42	JL1-LeafM01	XZBGJL1-0028	Figure S4, M	Blade linear, ~29 cm × 5 mm. Apex rounded. Margin entire. Secondary veins ~6 pairs, brochidodromous, 40° to midvein.			
43	JL1-LeafM02	XZBGJL1-0038	Figure S4, P	Blade elliptic, >43 mm × 25 mm. Margin entire. Secondary veins >6 pairs, eucampodromous, 45–60° to midvein. Interscedanaries prominent.			
44	JL1-LeafM03	XZBGJL1-0027, XZBGJL1-0032	Figure S4, Q	Leaf sessile. Blade lanceolate, ~37 mm × 10 mm. Base asymmetrical. Margin serrate. Secondary veins 7 pairs, semicraspedodromous, 45–60° to midvein. Interscedanaries prominent. Tertiary veins opposite percurrent.			
45	JL1-LeafM04	XZBGJL1-0013	Figure S4, U	Leaf petiolate. Blade elliptic, ~23–26 mm × 9–11 mm. Apex straight; Base decurrent. Margin entire. Secondary veins 3 pairs, hemieucampodromous, 30–35° to midvein.			
46	JL3-LeafM01	XZBGJL5-0003	Figure S5, E	Leaf petiolate. Blade lanceolate, ~50 mm × 8 mm. Apex acuminate; Base decurrent. Margin entire. Secondary veins ~14 pairs, brochidodromous, 45–60° to midvein. Tertiary veins reticulate.			
47	JL3-LeafM02	XZBGJL3-0012	Figure S5, H	Blade lanceolate, ~84 mm × 20 mm. Apex acuminate; Base decurrent. Margin entire. Secondary veins 11 pairs, hemieucampodromous, 45–50° to midvein. Interscedanaries prominent.			
48	JL3-LeafM03	XZBGJL3-0007	Figure S5, L	Blade lanceolate, ~58 mm × 16 mm. Apex acuminate; Base convex. Margin entire. Secondary veins 6 pairs, brochidodromous, 30–45° to midvein.			
49	JL4-LeafM01	XZBGJL4-0011	Figure S5, P	Blade elliptic, ~13 mm × 4 mm. Apex convex; Base convex. Margin entire. Secondary veins ~6 pairs, brochidodromous, 50–60° to midvein.			
50	JL5-LeafM01	XZBGJL5-0018	Figure S6, B	Leaf petiolate. Blade elliptic, ~18 mm × 6 mm. Apex straight; Base asymmetrical. Margin entire. Secondary veins 6 pairs, brochidodromous, 50–55° to midvein.			
51	JL5-LeafM02	XZBGJL5-0396, XZBGJL5-0525	Figure S6, E	Leaf petiolate. Blade linear, >75 mm × 6 mm. Base decurrent. Margin serrate. Secondary veins ~40 pairs, craspedodromous, 45° to midvein.			
52	JL5-LeafM03	XZBGJL5-0513	Figure S6, F	Blade lanceolate, ~45 mm × 7 mm. Margin entire. Secondary veins 6 pairs, brochidodromous, forming intramarginal secondary, 20° to midvein.			
53	JL5-LeafM04	XZBGJL5-0055	Figure S7, L	Leaf petiolate. Blade elliptic, ~38 mm × 20 mm. Base decurrent. Margin entire. Secondary veins >3 pairs, hemieucampodromous, 25–30° to midvein.			
54	JL5-LeafM05	XZBGJL1-0002, XZBGJL5-0519, XZBGJL5-0532	Figure S4, S; Figure S8, I	Leaf obovate-pinnately lobed with 5–6 pairs of leaflets. Blade ovate, ~20–30 mm × 6–12 mm. Apex acuminate; Base convex. Margin entire. Secondary veins 6–8 pairs, craspedodromous, 30–45° to midvein.			
55	JL5-LeafM06	XZBGJL5-0246	Figure S6, K	Leaf petiolate. Blade oblong-lanceolate, ~24 mm × 6 mm. Apex rounded; Base decurrent. Margin entire. Secondary veins ~9 pairs, brochidodromous, 40–45° to midvein.			
56	JL5-LeafM07	XZBGJL5-0086, XZBGJL5-0115, XZBGJL5-0380, XZBGJL5-0517	Figure S7, M	Leaf petiolate. Blade oblong, ~30 mm × 9 mm. Base decurrent. Margin entire. Secondary veins ~6 pairs, brochidodromous, 50–60° to midvein.			
57	JL5-LeafM08	XZBGJL5-0268, XZBGJL5-0270	Figure S6, M	Blade obovate, ~27 mm × 17 mm. Base convex. Margin serrate. Secondary veins 7 pairs, craspedodromous, 30–45° to midvein.			
58	JL5-LeafM09	XZBGJL5-0541	Figure S6, N	Blade elliptic, ~18 mm × 8 mm. Apex rounded; Base decurrent. Margin entire. Secondary veins 6 pairs, brochidodromous, 50–60° to midvein.			
59	JL5-LeafM10	XZBGJL5-0049	Figure S6, P	Blade elliptic, ~5 mm × 4 mm. Apex rounded; Base convex. Margin crenate. Secondary veins 4 pairs, semicraspedodromous, 45° to midvein. Tertiary veins irregular reticulate.			
60	JL5-LeafM11	XZBGJL5-0244	Figure S6, Q	Leaf petiolate. Blade lanceolate, ~85 mm × 21 mm. Base decurrent. Margin entire. Secondary veins 10 pairs, brochidodromous, 40° to midvein. Interscedanaries prominent. Tertiary veins abraded ramified.			
61	JL5-LeafM12	XZBGJL5-0235, XZBGJL5-0422	Figure S7, A	Leaf petiolate. Blade elliptic, ~80 mm × 22 mm. Apex acuminate; Base convex. Margin entire. Secondary veins ~12 pairs, brochidodromous, forming intramarginal secondary, 50–45° to midvein. Tertiary veins irregular reticulate.			
62	JL5-LeafM13	XZBGJL5-0390	Figure S7, B	Leaf petiolate. Blade elliptic, ~70 mm × 27 mm. Base convex. Margin entire. Secondary veins 10 pairs, brochidodromous, 60° to midvein. Interscedanaries prominent. Tertiary veins irregular reticulate. Higher-level veins irregular reticulate.			
63	JL5-LeafM14	XZBGJL5-0509	Figure S7, C	Leaf sessile. Blade lanceolate, ~68 mm × 22 mm. Base asymmetrical. Margin serrate. Secondary veins 17 pairs, semicraspedodromous, 45–70° to midvein. Interscedanaries prominent. Tertiary veins opposite percurrent.			
64	JL5-LeafM15	XZBGJL5-0542	Figure S7, D	Blade oblong, ~130 mm × 40 mm. Margin entire. Secondary veins ~8 pairs, brochidodromous, ~50° to midvein.			
65	JL5-LeafM16	XZBGJL5-0538, XZBGJL5-0539, XZBGJL5-0543	Figure S7, E	Leaf sessile. Blade oblong, ~60 mm × 22 mm. Base convex. Margin entire. Secondary veins >11 pairs, brochidodromous, forming intramarginal secondary, 40–55° to midvein. Interscedanaries prominent.			
66	JL5-LeafM17	XZBGJL5-0129, XZBGJL5-0521, XZBGJL5-0530	Figure S7, F	Leaf petiolate. Blade lanceolate, ~56 mm × 10 mm. Base decurrent. Margin entire. Secondary veins ~13 pairs, brochidodromous, 60° to midvein.			
67	JL5-LeafM18	XZBGJL3-0006, XZBGJL3-0014, XZBGJL3-0008, XZBGJL5-0139, XZBGJL5-0273, XZBGJL5-0279, XZBGJL5-0501	Figure S5, I; Figure S7, G	Leaf sessile. Blade lanceolate, ~85 mm × 12 mm. Apex rounded; Base asymmetrical. Margin entire. Secondary veins ~9 pairs, brochidodromous, 25–40° to midvein.			
68	JL5-LeafM19	XZBGJL5-0428	Figure S7, H	Blade lanceolate, ~78 mm × 13 mm. Apex acuminate. Margin crenate. Secondary veins 16 pairs, semicraspedodromous, 50–60° to midvein. Tertiary veins irregular reticulate.			
69	JL5-LeafM20	XZBGJL5-0516	Figure S7, J	Blade lanceolate, ~40 mm × 9 mm. Base convex. Margin entire. Secondary veins >8 pairs, brochidodromous, 40–55° to midvein.			
70	JL5-LeafM21	XZBGJL5-0326, XZBGJL5-0373, XZBGJL5-0404	Figure S7, K	Blade oblong, ~16 mm × 4 mm. Apex convex. Margin entire. Secondary veins ~5 pairs, brochidodromous, forming intramarginal secondary, 30–35° to midvein. Tertiary veins irregular reticulate.			

**Table S3.** Paleoclimate reconstruction of the Jianglang flora using Climate-Leaf Analysis Multivariate Program (CLAMP). MAT- mean annual air temperature, WMMT - warm month mean air temperature, CMMT - cold month mean air temperature, LGS - length of the growing season, GSP - growing season precipitation, MMGSP - mean monthly growing season precipitation, 3WET - precipitation in the three consecutive wettest months, 3DRY - precipitation in the three consecutive driest months, RH - mean annual relative humidity, SH - mean annual specific humidity, ENTHAL - mean annual moist enthalpy, VPD.Ann - mean annual vapor pressure deficit, VPD.Win - mean vapor pressure deficit during winter (DJF), VPD.Spr - mean vapor pressure deficit during spring (MAM), VPD. Sum - mean vapor pressure deficit during summer (JJA), VPD.Aut - mean vapor pressure deficit during fall (SON), THERM - mean annual thermicity, MINT.Wrm -mean minimum temperature of the warmest month, MAXT.Cld - mean maximum temperature of the coldest month mean, GDD0 - growing degree days above 0 °C, GDD5 - growing degree days above 5 °C, PET.Ann - mean annual potential evapotranspiration, PET.Wrm - mean evapotranspiration during the warmest month, PET.Cld - mean potential evapotranspiration during the coldest month.

	MAT	WMMT	CMMT	GROWSEAS	GSP	MMGSP
	(°C)	(°C)	(°C)	(months)	(9)	(9)
Jiangling	18.89	28.67	7.42	11.01	208.89	21.02
SD	2.36	2.91	3.54	1.09	64.32	6.50
	3WET	3DRY	RH	SH	ENTHAL	VPD.Ann
	(9)	(9)	(%)	(g/kg)	(kJ/kg)	(hPa)
Jianglang	100.36	17.62	57.05	8.64	32.59	10.52
SD	40.04	9.82	10.14	1.77	0.84	2.35
	VPD.Win	VPD.Spr	VPD.Sum	VPD.Aut	THERM	MINT.Wrm
	(hPa)	(hPa)	(hPa)	(hPa)	(°C)	(°C)
Jianglang	5.60	10.06	14.77	10.81	387.01	22.44
SD	1.52	3.95	3.47	2.01	74.90	2.94
	MAXT.Cld	GDD0x10 <sup>-3</sup>	GDD5x10 <sup>-3</sup>	PET.Ann	PET.Wrm	PET.Cld
	(°C)			(mm/dayx10 <sup>-1</sup> )	(mm/day)	(mm/day)
Jianglang	14.39	82.61	85.31	129.15	159.19	45.82
SD	3.54	11.80	10.61	16.64	24.50	14.02

**Table S4.** Spreadsheet showing how the latitudinal correction between model and proxy for moist enthalpy was achieved and then how the paleoelevation was calculated. The differences between model-estimated moist enthalpies and those derived from the CLAMP proxy for middle Eocene leaf assemblages spanning a wide paleolatitudinal range were plotted against paleolatitude. This gave a latitude-dependent linear regression that provided a correction (-1.66 kJ/kg) at the paleolatitude of the Jiangliang flora (22.5°N). Because this regression indicated that the difference underestimated moist enthalpy at the Jiangliang site by 1.66 kJ/kg, this value was added to the model predicted sea level moist enthalpy at the Jiangliang site. The CLAMP-derived moist enthalpy was then subtracted from it to give the moist enthalpy difference between sea level and the paleoelevation of the Jiangliang flora, and this value was then divided by g to obtain an elevation of 1.5 km.

Parameter	Jiangliang	Gurha_1	Gurha_2	Svalbard	Puget9694	Puget9731	Puget9833	Puget9678
Model M.S.L. Moist Enthalpy (kJ/kg)	339.00	364.70	364.70	289.77	313.42	313.42	313.42	313.42
CLAMP Moist Enthalpy (kJ/kg)	325.90	353.38	353.30	324.36	340.70	340.60	338.90	336.20
Paleolatitude (°N)	22.50	5.32	5.32	73.25	53.70	53.70	56.20	53.70
Moist Enthalpy Difference (kJ/kg)	13.10	11.31	11.40	-34.59	-27.28	-27.18	-25.48	-22.78



Residuals		-0.28	-0.36	-0.07	5.77	5.67	2.29	1.27
Standard Dev of Residuals	2.687956							
Jiangliang sea level moist enthalpy adjustment		-1.66 kJ/kg						
Jiangliang Paleoelevation		1.50 km						
Combined CLAMP and 'correction' uncertainty		0.90 km						



## SI References

1. H. Tang *et al.*, Extinct genus *Lagokarpos* reveals a biogeographic connection between Tibet and other regions in the Northern Hemisphere during the Paleogene. *J. Syst. Evol.* **57**, 670–677 (2019).
2. J. Liu *et al.*, Biotic interchange through lowlands of Tibetan Plateau suture zones during Paleogene. *Palaeogeogr. Palaeoclimatol. Palaeoecol.* **524**, 33–40 (2019).
3. C. Del Rio *et al.*, *Asclepiadospermum* gen. nov., the earliest fossil record of Asclepiadoideae (Apocynaceae) from the early Eocene of central Qinghai-Tibetan Plateau and its biogeographic implications. *Am. J. Bot.*, **107**, 126–138 (2020).
4. R. A. Spicer *et al.*, Why the 'uplift of the Tibetan Plateau' is a myth. *Natl. Sci. Rev.* <https://doi.org/10.1093/nsr/nwaa091> (2020).
5. P. Kapp, P. G. DeCelles, Mesozoic-Cenozoic geological evolution of the Himalayan-Tibetan orogen and working tectonic hypotheses. *Am. J. Sci.* **319**, 159–254 (2019).
6. A. Farnsworth *et al.*, Past East Asian monsoon evolution controlled by paleogeography, not CO<sub>2</sub>. *Sci. Adv.* **5**, eaax1697 (2019).
7. Z. Xiong *et al.*, The early Eocene rise of the Gonjo Basin, SE Tibet: From low desert to high forest. *Earth Planet. Sci. Lett.* **543**, 116312 (2020).
8. A. K. Laskowski, D. A. Orme, F. Cai, L. Ding, The Ancestral Lhasa River: A Late Cretaceous trans-arc river that drained the proto-Tibetan Plateau. *Geology* **47**, 1029–1033 (2019).